 DOI: 10.1002/masy.201100178

Fluorescent-Magnetic Nanostructures Based on Polymer-Quantum Dots Conjugates

Maria I. N. da Silva,[1] *Alexandra A. P. Mansur,*[1] *Vanessa Schatkoski,*[1] *Klaus W. H. Krambrock,*[2] *Juan González,*[2] *Herman S. Mansur**[1]

Summary: In this study it is presented the synthesis and the characterization of Fluorescent-Magnetic Nanostructures based on polymer-quantum dots conjugates. Polyvinyl alcohol (PVA) was used as the capping-ligand for the preparation of $Cd_xMn_{1-x}S$ semiconductor nanocrystals via aqueous colloidal chemistry. Different substitution ratios of Cd^{2+} by Mn^{+2} ions were investigated aiming at the formation of stable nanoparticles with photo-luminescent and semi-magnetic properties. UV-visible spectroscopy (UV-vis), photoluminescence spectroscopy (PL), Electric Paramagnetic Resonance Spectroscopy (EPR), and transmission electron microscopy (TEM) were used to characterize the formation and the relative stability of $Cd_xMn_{1-x}S$ nanoparticles. The results have showed the influence of the Mn^{2+}partially replacing Cd^{2+} in the optical behavior of the quantum dots (QDs) produced. In addition, the $Cd_xMn_{1-x}S$ QDs have evidenced luminescent and semi-magnetic properties. Thus, the biocompatible water-soluble polymer was effective as ligand for synthesizing and stabilizing QDs conjugates with properties allowing them to be potentially applied as imaging and labeling probes in the biomedical field.

Keywords: biological applications of polymers; colloids; conjugated polymers; nanocomposites; nanoparticles; quantum dots; water-soluble polymers

Introduction

Polymer science has become a field of intense research aiming at moving from conventional usage towards advanced materials, principally in bio-nanotechnology. The possibility of combining polymers with other materials is a topic practically with unlimited opportunities.[1–4] Over the past several years, polymer nanocomposites and hybrids conjugated with inorganic components have been considered promising systems for bio-medical applications, such as drug delivery, biosensors, diagnostic tools and as imaging probes. In that sense, semiconductor nanocrystals or quantum dots (QDs) have attracted much attention because their optical, electronic and magnetic properties are known to be size-dependent.[1–7] The alternative of joining biocompatible polymers with quantum dots has a remarkable potential in labeling biological entities such as cells, tissues and organs for medical diagnostics and targeted therapeutics.[1–5] Advanced properties such as higher quantum efficiency, good photostability and magnetic properties in the luminescent QDs offer the perspective for the development of a new class of luminescent biomarkers surpassing the organic fluorescent dyes. Type (II–VI) semiconductors (i.e. MX, M = Cd, Pb, Zn; X = S, Se, Te) have been the most frequent choice for producing quantum dots. Recently, transition metal ions doped II–VI nanoparticles have drawn much interest

[1] Department of Metallurgical and Materials Engineering, Federal University of Minas Gerais, Av. Antônio Carlos, 6627, School of Engineering, Pampulha, Belo Horizonte/MG, 31.270-901, Brazil
Fax: ++55 31 34091815;
E-mail: hmansur@demet.ufmg.br
[2] Department of Physics, Federal University of Minas Gerais, Brazil

because they can improve and modify the optical features and may also add magnetic properties.[8–10] Among the possible magnetic impurities that may be introduced into a II-IV compound semiconductor lattice, Mn plays a special role because of the $3d^5 4s^2$ configurations of the spins in a free atom. The divalent Mn (Mn^{2+}) can easily substitute metal cations (Cd^{2+}) in the nanocrystal host lattice, and has an appropriate solubility in chalcogenides (S, Se, Te).[8–10] Besides, it has been reported that the magnetic properties of $Cd_xMn_{1-x}S$ nanocrystals are noticeably enhanced compared to those observed in the bulk phase.

Hence, in this work, $Cd_xMn_{1-x}S$ quantum dots were prepared using a colloidal aqueous route at room temperature using PVA as polymeric stabilizing agent and the effects of Cd^{2+}/Mn^{2+} ratio in the optical and magnetic properties of QDs were investigated. Despite some studies, to the best of our knowledge this is the first report where these PVA-Quantum dots conjugates in colloidal solution were successfully produced and extensively characterized regarding to their dimensions, fluorescent and semi-magnetic properties.

Experimental Part

$Cd_xMn_{1-x}S$ were synthesized using an aqueous colloidal dispersion as a result of the reaction between cadmium perchlorate ($Cd(ClO_4)_2.6H_2O$, Aldrich), manganese sulfate ($MnSO_4$, VETEC), and thioacetamide (CH_3CSNH_2, Aldrich). Poly(vinyl alcohol), PVA, with high degree of hydrolysis (DH > 99.3%, Aldrich) and average molecular weight (Mw) 85.000–124.000 $g.mol^{-1}$ was used as capping-ligand agent for the nanoparticle chemical stabilization. Deionized water (DI-water, Millipore Simplicity™) with the resistivity of 18 MΩ.cm was used in the preparation all solutions.

The synthesis was carried out similar to the previously reported procedure.[2,3,5] Briefly, 2 mL of PVA solution (1.0 $mol.L^{-1}$) and 45 mL of DI water were added to the flask reacting vessel. Under moderate magnetic stirring, the pH was adjusted to 11.75 with a solution of NaOH (1.0 $mol.L^{-1}$, Merck). Next, considering the general stoichiometric proportion of $Cd_xMn_{1-x}S$, it was added the calculated volumes of cadmium precursor solution (V_{Cd}, 1.0×10^{-2} $mol.L^{-1}$), manganese solution (V_{Mn}, 1.0×10^{-2} $mol.L^{-1}$; $V_{Mn} = 4.0 - V_{Cd}$ mL) and 2.5 mL of thioacetamide solution used as sulfide precursor (8.0×10^{-3} $mol.L^{-1}$). In the final solution, the total amount of moles of cations ($[Cd^{2+}] + [Mn^{2+}]$) were kept constant and equal to 4.0×10^{-5} mol. Therefore, the calculated number of moles of anions [S^{-2}] was equal to 2.0×10^{-5} mol, resulting on the final molar ratio of 2:1 (cation: anion). The values of Mn molar fraction (1-x) under evaluation and the respective V_{Cd} volume are showed in Table 1, with the molar fraction "x" varying from 0% (x = 0.0, pure Cd^{2+}) to 100% (x = 1.0, pure Mn^{2+}). The synthesis is relatively facile and typically takes less than 4 h for the entire process. UV-visible spectroscopy (UV-vis), Photoluminescence spectroscopy (PL), Transmission Electron Microscopy (TEM), and Electric Paramagnetic Resonance Spectroscopy (EPR) were used to characterize the $Cd_xMn_{1-x}S$ quantum dots. The UV-vis spectroscopy

Table 1.
Table of experiments for the synthesis of $Cd_xMn_{1-x}S$ nanoparticles.

[Cd] (x)	[Mn] (1-x)	Volume Cd^{+2} (V_{Cd}) (mL)	Volume Mn^{+2} (V_{Mn}) (mL)	Sample identification
1.00	0	4.0	0.0	CdS
0.75	0.25	3.0	1.0	$Cd_{0.75}Mn_{0.25}S$
0.50	0.50	2.0	2.0	$Cd_{0.50}Mn_{0.50}S$
0	1.00	0	4.0	MnS

was used for evaluating the reaction of the formation of QDs and their relative colloidal stability in the PVA-water medium. The UV-Vis absorption measurements were conducted using a Perkin Elmer equipment (Lambda EZ-210, transmission mode), wavelength ranging from 700 nm to 300 nm, with a quartz cuvette (10 mm path-length). Photoluminescence emission spectra were acquired using an Ocean Optics USB4000 VIS-NIR spectrophotometer and a Helium-Cadmium (He:Cd) laser at $\lambda = 442$ nm (violet-blue, 15 mW of power) as the excitation source. Also, QDs colloidal media were placed inside a ''darkroom-chamber'' at room temperature where they were illuminated by UV radiation emission bulb ($\lambda_{excitation} =$ 245 nm, 6W, Boitton Instruments). Digital color images were collected as the QDs fluoresce in the visible range of the spectra. The nanostructural characterizations of the $Cd_xMn_{1-x}S$ nanoparticles, based on the captured digital images, were performed using a Tecnai G2-20-FEI transmission electron microscope (TEM) at an accelerating voltage of 120 kV. Samples were prepared by dropping the colloidal solution over a holey carbon grid after a purification step. Purification was carried out using an ultra-centrifugal device with 60.000 Mw cut-off cellulose membranes (Amicon filter, Millipore). Centrifugation was conducted for 30 min (6 cycles x 5 min per cycle, at 12000 r.p.m.) using a Hettich Mikro 200R centrifuge. After the first cycle, it was washed 5 times with 400 μL DI-water. Centrifugal forces removed the excess of reagents. The size and the size distribution data were obtained by measuring over than 500 individual nanoparticles using an image processing program (ImageJ, version 1.44, public domain, National Institute of Mental Health). EPR spectroscopy was utilized to access the magnetic properties of the nanocrystals for the alloys of $Cd_xMn_{1-x}S$. EPR spectra were recorded at room temperature on a laboratory-built heterodyne spectrometer with a 500 mW klystron (Varian), a commercial cylindrical resonance cavity (Bruker) and an electromagnet (Varian) with maximum field amplitude of 500 mT.

Results and Discussion

In Figure 1 it is presented the schematic representation of the produced quantum-dots conjugated to PVA. It is expected that the nucleation and further growth of the nanocrystals was limited by the capping behavior of the polymer chain, mostly due to the interactions between hydrophilic groups from PVA and Cd^{2+} at the QDs surfaces.[2,3,5]

Some essential concepts are required to better understand the conjugation of QDs with polymers. In short, it is widely known that semiconductor nanoparticles made from metal chalcogenides (II-IV) and alloys exhibit a very distinct change in their optical absorption properties when their sizes are reduced below a certain threshold dimension.[1–2] However, due to the extremely small size of the nanocrystals a capping reagent must be added to achieve a stable colloidal dispersion. Therefore, PVA was used as the ligand for limiting the size of $Cd_xMn_{1-x}S$ colloidal nanocrystals. The system stability and dimension of QDs were accessed by UV-visible spectroscopy technique. In Figure 2, the UV-vis absorption spectra have evidenced relevant changes mostly in the region varying from 450 nm to 600 nm. This behavior was assigned to the optical transition of the excitonic state, i.e. this absorption band was related to the first optically allowed transition of $Cd_xMn_{1-x}S$ between the electronic state in the conduction band (C_B) and hole state in the valence band (V_B).[2–5,8,9]

The average size of semiconductor nanoparticles can be estimated by the optical band gap from absorption coefficient data as a function of wavelength using the Tauc relation,[11] as showed in Eq. 1:

$$\alpha h\upsilon = A(h\upsilon - E_{g,QD})^{1/2} \quad (1)$$

Where A is a relative constant for the material, $E_{g,QD}$ (eV) is the optical band gap

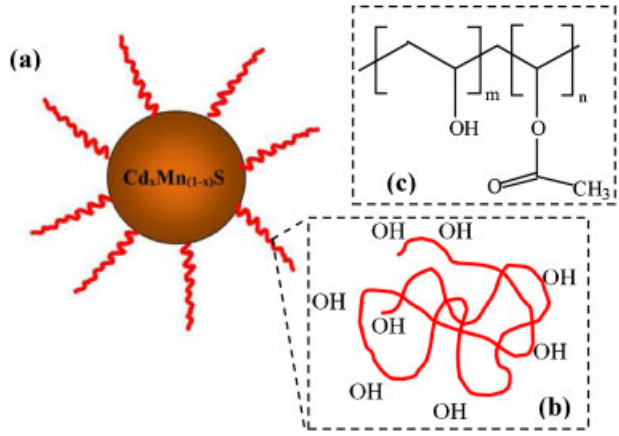

Figure 1.
Schematic representation of the produced quantum-dots conjugated to PVA (a). Detail: PVA polymer chain with hydroxyls as main functional chemical groups (b); PVA chemical structure with acetates and alcohol units (c).

of the nanoparticles, α is the absorption coefficient and hυ is the photon energy. Hence, the values of optical band gap can be obtained from the plots of $(\alpha h\upsilon)^2$ versus hυ and extrapolating the straight portion of the graph to hυ, i.e. at $\alpha = 0$ as showed in Figure 2 (insert). Next, the sizes of quantum dots were calculated using Brus equation[12] and the results are summarized in Table 2. It can be noted that, by varying the relative stoichiometric ratio of Cd^{2+}/Mn^{2+} in the $Cd_xMn_{1-x}S$ quantum dots, it was possible to change the average size ranging from 3.3 nm to 4.1 nm. Moreover, the diameter of the $Cd_xMn_{1-x}S$ quantum dots ($x > 0$) increased as the concentration of Mn^{2+} was raised with the consequent reduction in the band gap energy. As all energy values were higher than the CdS "bulk" energy (~2.4 eV), referred as "blue-shift", it can

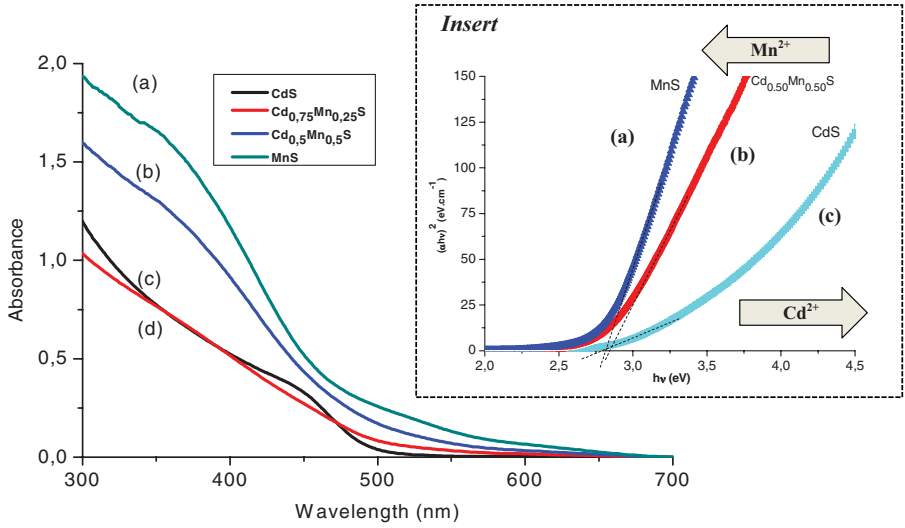

Figure 2.
UV-Vis spectra of $Cd_xMn_{1-x}S$ with varying the Mn^{2+} concentrations (a) MnS, $x = 0$; (b) $Cd_{0.5}Mn_{0.5}S$, $x = 0.50$; (c) CdS, $x = 1.0$; (d) $Cd_{0.75}Mn_{0.25}S$, $x = 0.75$; (insert) Optical band gap energy: (a) MnS, (b) $Cd_{0.50}Mn_{0.50}S$, (c) CdS.

Table 2.
$Cd_xMn_{1-x}S$ quantum dots: band gap energy and average diameter.

$Cd_xMn_{1-x}S$	Band gap energy $E_{g,QD}$ (eV)	Average diameter (nm)
CdS	2.77	4.1
$Cd_{0.75}Mn_{0.25}S$	3.04	3.3
$Cd_{0.50}Mn_{0.50}S$	2.85	3.8
MnS	2.83	3.9

be affirmed that the $Cd_xMn_{1-x}S$ quantum dots were synthesized in the quantum confinement regime.[1,2,8,9,12]

The morphology, nanoparticle size and size distribution of $Cd_xMn_{1-x}S$ quantum dots conjugated to PVA were characterized by TEM. As it can be observed in the typical TEM image collected of CdS system (Figure 3a and Figure 3b), the quantum dots were produced and stabilized with PVA polymer with average diameters within the range of 3.0 to 5.0 nm (Figure 3c). They were obtained via aqueous colloidal route and, during sample preparation for TEM analysis, they have formed agglomerates and clusters. Nevertheless, the histogram of nanoparticle size distribution (Figure 3d) has indicated the average diameter of about 3.4 nm. These results are consistent with the sizes determined based on the optical band gap discussed in the previous section. In Figure 3c is showed the selected-area electron diffraction image (SAED) of the CdS quantum dots with estimated plane spacing dimensions.

In order to be used as fluorophores, the quantum dots must present photoactivity when submitted to radiative excitation. Thus, the PL spectra of the $Cd_xMn_{1-x}S$ quantum dots are showed in Figure 4. As a general trend, all samples have exhibited a broad band ranging from approximately 450 nm to 800 nm, centered at 620–650 nm. It has been reported that nanocrystals of CdS have luminescence in the blue, green, orange and red regions of the spectra.[2,5,8–10] Blue luminescence is associated with the excitonic emission and it was observed for CdS at 485 and 495 nm. These peaks are shifted to higher wavelength regions of the PL spectra relative to the position of the absorption band due to a Stokes shift.

In the green spectral region, a sharp band at 520 nm was detected in CdS sample and blue shifted to lower wavelength (513 nm) with the increase of Mn^{2+} molar fraction in the $Cd_xMn_{1-x}S$ nanoparticles. The $Cd_xMn_{1-x}S$ quantum dots were synthesized with the cation:anion ratio maintained at 2:1, which has favored the excess of metal ions to entering into the lattice at interstitial

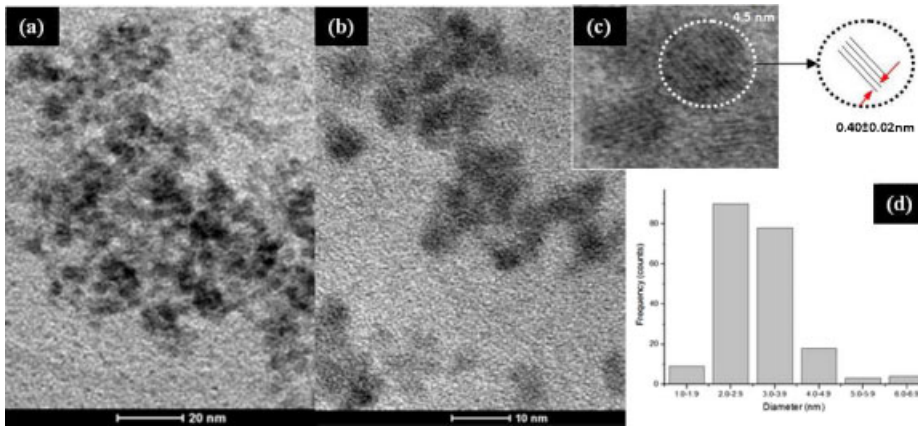

Figure 3.
TEM images of CdS ($x = 1$, $Mn^{2+} = 0$) quantum dots, (a) and (b). Selected-area electron diffraction image-SAED (c). Histogram of nanoparticles size distribution (d).

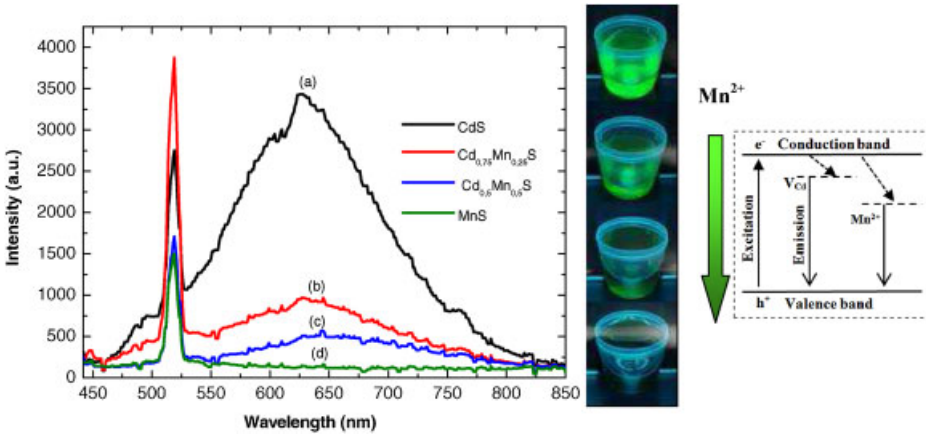

Figure 4.
PL spectra of $Cd_xMn_{1-x}S$ quantum dots (a) CdS; (b) $Cd_{0.75}Mn_{0.25}S$; (c) $Cd_{0.5}Mn_{0.5}S$; (d) MnS. Detail: Digital images of green luminescence of $Cd_xMn_{1-x}S$ quantum dots excited with UV lamp, $\lambda_{excitation} = 245$ nm); Drawing of the band structure of quantum dots under excitation followed by different emission pathways.

sites (Cd_i or Mn_i). Orange luminescence (590–625 nm) is observed in the case when interstitial atoms of metal are present in the lattice of semiconductor. That is often verified with nanocrystals exhibiting luminescence at about 519 nm.

Finally, the red band of PL is typically observed in the nanoparticles which contain a certain concentration of intrinsic defects of the type V_{Cd}-V_s. Moreover, the relevant reduction in the peak at 625 nm when the Mn^{2+} concentration was raised can be attributed to the partial replacement of Cd^{2+} by Mn^{2+}.[8,9] A major distinction between the CdS:Mn systems reported by other authors and the one presented in this work is related to the synthesis process of the polymer-QDs conjugates. For instance, the precursors and stabilizer/surfactant are entirely different and the reaction was conducted at room temperature without any heat-treatment for annealing. Essentially, the occurrence of "deep traps" (internal defects) associated with the "shallow surface states" of the nanocrystals will act as traps of excited carriers. As a result, the PL behavior will be determined by the contribution of all these parameters and, therefore it cannot be compared straightforwardly to others.[8,9,13,14] In spite of the often reported low photoactivity of nanocrystals obtained by aqueous routes, it should be highlighted that the new $Cd_xMn_{1-x}S$ quantum dots produced in this work using PVA ligand have unquestionably behaved as active fluorophores under excitation.

The addition of divalent Mn ions in the CdS quantum dots ($Cd_xMn_{1-x}S$) aimed at developing a novel class of nanomaterials with optical fluorescence associated with semi-magnetic properties. The manganese atom has an electronic configuration of $[Ar]3d^54s^2$ suitable for the partial substitution of transition metals such as cadmium in crystalline semiconductors.[8,9] So, when Mn^{2+} is introduced into CdS nanocrystals, it is probable that some replacement of Cd^{2+} sites may occur. In that sense, the characterization of these nanocrystals using Electric Paramagnetic Resonance (EPR) was carried out and a typical result for the $Cd_{0.50}Mn_{0.50}S$ quantum dots is showed in Figure 5. The EPR spectrum presented the overall profile consistent with the literature concerning to paramagnetic materials.[15–19] The well-defined six line spectrum (insert of Figure 5) with a line width of about $\Delta H = 10$ mT is a characteristic of the Mn^{2+} in tetrahedral cationic substitution site, dispersed into the CdS matrix.[15–19]

These results are of paramount importance as far as the magnetic properties are

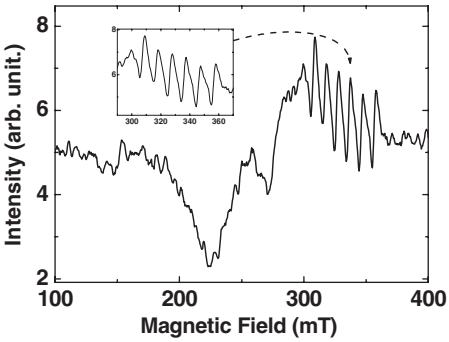

Figure 5.
EPR spectrum of the $Cd_{0.50}Mn_{0.50}S$ quantum dots. Insert: Hyperfine structure of the diluted Mn in CdS lattice.

concerned, because they gave supporting evidence that the Mn^{2+} altered the hyperfine band structure of CdS QDs. Therefore, the designed substitution of Cd^{2+} sites with Mn^{2+} in the semiconductor lattice has produced diluted type of alloyed quantum dots ($Cd_xMn_{1-x}S$) with luminescent properties associated with potential semi-magnetic behavior.

Conclusions

Novel semiconductor nanoparticles of $Cd_xMn_{1-x}S$ were successfully synthesized using poly(vinyl alcohol) as stabilizing agent via aqueous colloidal chemistry. The results have clearly showed the influence of Mn^{2+} partially replacing Cd^{2+} in the optical and magnetic behaviors of the quantum dots produced. Moreover, the transmission electron microscopy images have endorsed the average size of QD in the range of 3–4 nm estimated by UV-visible spectroscopy and also without any indication of segregation or phase separation caused by the amount of Mn^{+2} added to the CdS lattices. Electron paramagnetic resonance measurements revealed Mn^{2+} sites within the matrix of the $Cd_xMn_{1-x}S$ nanocrystals causing semi-magnetic response. Finally, based on the results it can be stated that $Cd_xMn_{1-x}S$/PVA conjugates have evidenced PL and semi-magnetic properties suitable for potential applications as probes and bio-markers in biology and medicine areas.

Acknowledgements: The authors acknowledge the financial support from CAPES, FAPEMIG, and CNPq. The authors also would like to acknowledge to the Center of Microscopy at the Federal University of Minas Gerais for TEM experiments.

[1] H. S. Mansur, *WIREs Nanomedicine and Nanobiotechnology* **2010**, *2*, 113.
[2] H. S. Mansur, A. A. P. Mansur, J. C. González, *Polymer* **2011**, *52*, 1045.
[3] H. S. Mansur, A. A. P. Mansur, *Mater. Chem. Phys.* **2011**, *125*, 709.
[4] H. S. Mansur, A. A. P. Mansur, J. C. González, *Colloid Surface B* **2011**, *84*, 360.
[5] A. Mansur, H. Mansur, J. González, *Sensors* **2011**, *11*, 9951.
[6] H. S. Mansur, A. A. P. Mansur, *J. Mater. Chem.* **2012**, *22*, 9006.
[7] H. S. Mansur, W. L. Vasconcelos, F. Grieser, F. Caruso, *J. Mater. Sci.* **1999**, *34*, 5285.
[8] S. Liu, F. Liu, H. Guo, *Solid State Commun.* **2000**, *115*, 615.
[9] R. Beaulac, P. I. Archer, D. R. Gamelin, *J. Solid State Chem.* **2008**, *181*, 1582.
[10] V. I. Fediv, A. I. Savchuk, V. M. Frasunyak, V. V. Makoviy, O. A. Savchuk, *J. Phys.: Conf. Ser.* **2010**, *245*, 012084.
[11] J. Tauc, A. Menth, *J. Non-Cryst. Solids* **1972**, *8–10*, 569.
[12] L. E. Brus, *J. Chem. Phys.* **1984**, *80*, 4403.
[13] R. Koole, W. J. M. Mulder, M. M. van Schooneveld, G. J. Strijkers, A. Meijerink, K. Nicolay, *WIREs Nanomedicine and Nanobiotechnology* **2009**, *1*, 475.
[14] S. Ghosh, A. Mukherjee, H. Kim, C. Lee, *Mater. Chem. Phys.* **2003**, *78*, 726.
[15] B. Sambandam, N. Rajendran, M. Kanagaraj, S. Arumugam, P. T. Manoharan, *J. Phys. Chem. C* **2011**, *115*, 11413.
[16] H. T. Xue, P. Q. Zhao, *J. Phys. D: Appl. Phys.* **2009**, *42*, 015402.
[17] M. A. Malik, P. O'Brien, N. Revaprasadu, *J. Mater. Chem.* **2001**, *11*, 2382.
[18] B. Babić-Stojić, D. Milivojević, V. V. Vodnik, M. I. Čomor, *Mater. Sci. Forum* **2004**, *453–454*, 263.
[19] S. Bhattacharyya, Y. Estrin, D. H. Rich, D. Zitoun, Y. Koltypin, A. Gedanken, *J. Phys. Chem. C* **2010**, *114*, 22002.

